Z. Phys. C 63, 637–650 (1994)

ZEITSCHRIFT
FÜR PHYSIK C

Quantum number conservation in statistical models and its application to $p\bar{p}$-annihilation at rest

Wolfgang Blümel[1,*], Peter Koch[2,**], Ulrich Heinz[3,***]

[1]Institut für Theoretische Physik, Universität Regensburg, D-93040 Regensburg, Germany
[2]Institut für Theoretische Physik, Universität Bremen, D-28334 Bremen, Germany
[3]Institute for Theoretical Physics, University of California, Santa Barbara, CA 93106–4030, USA

Received: 30 September 1993 /In revised form: 18 January 1994

Abstract. We investigate the role of exact quantum number conservation in small statistical systems and illustrate the consequences for $p\bar{p}$-annihilation at rest. A group theoretical projection method is used to calculate a restricted canonical partition function which consists only of states allowed by the conservation laws. Special emphasis is put on the conservation of isospin, total angular momentum, and C-, G-, and P-parities. Our analysis of the partition function shows that it is increasingly dominated by two-particle states as more of the conservation laws are included. The constraining effects on various multiplicity ratios and the deviations from the unconstrained limit are discussed in detail.

1 Introduction

Compared with the well-studied NN system, the interaction in the $N\bar{N}$ system is quite different since, due to the vanishing total baryon number, it is dominated by annihilation into multi-meson final states. Attempts to derive the dynamics of this annihilation process from the underlying principles of quantum chromodynamics have not been very successful up to now. Since the relevant length scale for the annihilation process is of the order of 1 fm, nonperturbative effects dominate and a rigorous theoretical description is not yet possible. As a consequence the experimental data are usually analyzed on the basis of more or less phenomenological models, of which the most popular ones are based on static potentials with a strong imaginary part, on statistical concepts or on the constituent quark model.

A typical annihilation event at rest produces on the average 5 pions with a momentum distribution which to a good approximation can be represented by a Boltzmann distribution [1, 2]. This observation, combined with the lack of knowledge about the fundamental theory of strong interactions, led in the early days of $N\bar{N}$ physics to the idea that the annihilation process proceeds through an intermediate state where microscopic details of the interaction process are not important and in which all information on the initial state is lost. This intermediate state was thought to resemble very closely an ideal quantum gas consisting of essentially non-interacting mesons and their resonances. Each final state particle should then appear according to its statistical weight factor, and the only constraints imposed on the system would originate from the requirement of conservation of some specific quantum numbers like electric charge Q, baryon number B, etcetera.

In most cases the ideas developed by Koppe [3] and Fermi [4], which were first applied in the late forties to pion-nucleon and nucleon-nucleon collisions, were simply taken over to the case of $N\bar{N}$ annihilation. Surprisingly, these simple models produced rather good results in describing pion multiplicities, momentum spectra and branching ratios (see, e.g., [5–8], and the survey of the early works given in [9]).

With the advent of the low energy anti-proton accelerator (LEAR) at CERN and the ability to make quite precise exclusive measurements of the final state, the existence of dynamical correlations beyond a purely statistical description has been firmly established [10, 11]. As a consequence, models have been developed which, in contrast to purely statistical concepts, assume a well defined intermediate state [12–15].

On the basis of these exclusive measurements it is nowadays widely believed (at least for annihilation at rest) that annihilation can be effectively described by quasi two- and three-body final state channels. Based on this assumption, theoretical analyses of $p\bar{p}$ annihilation into mesons have been carried out in the framework of quark rearrangement and/or quark-antiquark annihilation [12, 14]. But even though a large part of the experimental data can be sufficiently well described by such models, they do not provide a precise and complete understanding of the annihilation amplitude.

*Supported by DFG
**Supported in part by BMFT and DFG
***Permanent address: Institut für Theoretische Physik, Universität Regensburg, D-93040 Regensburg. Work supported in part by DFG, BMFT and GSI

In view of the successes and limitations of these attempts for a microscopic understanding of the annihilation process, the main interest in a statistical approach to $N\bar{N}$ has nowadays turned to the question, which quantities, channels or other features of a $N\bar{N}$ annihilation system are dominated by statistics and general conservation laws, and which are governed by microscopic details of the interaction mechanism which go beyond the statistical approach. Of course, a satisfying answer to this question requires a proper treatment of all the relevant selection rules together with the underlying symmetries also within the statistical approach to $p\bar{p}$ annihilation.

Early developments in the framework of the microcanonical ensemble concentrated on the question how the conservation of characteristic quantum numbers, like for example isospin [16–18], should be incorporated into the statistical description. In contrast to this only very few attempts have been made to include also the conservation of angular momentum [19, 20], which in case of $N\bar{N}$ annihilation is now known to play a very important role [10, 11, 21–23]. Owing to the rather complicated and cumbersome nature of computations within the microcanonical approach, no detailed investigation of the influence of angular momentum conservation (AMC) for multiparticle production in hadronic interactions exists so far.

During the last decade, however, very useful group theoretical methods have been developed which allow in a relatively simple way for the exact conservation of quantum numbers in the framework of the *canonical* or *grand canonical ensemble* [24–28], which from the technical point of view are much easier to handle. Although one might be worried about using such a picture for the description of a system which contains only 5 particles on the average, the known exponential behaviour of the pion momentum spectrum, when averaged over many events, suggests the introduction of a temperature [26, 29]. Furthermore, since in $N\bar{N}$ annihilation the amount of energy available for particle pair-creation is rather big compared to the particle masses, the grand canonical ensemble with a vanishing chemical potential will be employed throughout this work.

Following this line, we will present in Sect. 2 our statistical model in a grand canonical description, where energy and momentum are conserved on the average while all other relevant quantum numbers, as there are isospin, P, C and G parity, strangeness, and baryon number are conserved *exactly*. Special emphasis will be put on the group theoretical implementation of exact angular momentum conservation. In Sect. 3 we analyze the $\bar{p}p$-annihilation at rest and elaborate in more detail on the impact of the conservation laws, particularly of AMC, followed by a discussion of predicted mean multiplicities and a comparison with experimental data.

2 The projection operator formalism in a thermodynamical model

2.1 General method

It is well known, that the macroscopic properties of a statistical system can be described by the microcanonical, canonical or grand canonical ensembles. While in the thermodynamic limit ($V \to \infty$, $N/V = \text{const.}$) all three descriptions lead to identical results, they differ for small systems. Whereas in the microcanonical approach energy, volume and all conserved quantum numbers are fixed exactly, the canonical approach allows for statistical fluctuations of the total energy, which is thus conserved only on the average, with the temperature T as the quantity controlling the distribution of energy among the degrees of freedom. In the grand canonical approach the latter is true for all other conserved quantum numbers. Since the relative importance of the fluctuations is proportional to $1/\sqrt{N}$ where N is the number of particles in the system, small systems are strongly influenced by these fluctuations. In the case of conserved quantum numbers these fluctuations are unphysical and may thus lead to serious qualitative errors in the calculation of certain macroscopic observables. Hence they should be excluded, i.e. the canonical or microcanonical description should be used rather than the grand canonical one.

On the other hand calculations in the grand canonical formalism are technically very much simpler than in the other two approaches. This led to the introduction of projection techniques into statistical approaches, which allow to project out the unwanted unphysical quantum number fluctuations from the grand canonical partition function (equivalent to removing from the sum all states forbidden by selection rules) without giving up most of its technical ease. Among the first to apply such a technique were Magalinskii and Terletskii [30], and a general group theoretical foundation was later given by Turko and Redlich [24, 25]. In the latter formulation one writes down a "generating function"

$$\tilde{Z}(T, V, \boldsymbol{\alpha}) = \sum_{\Gamma} \frac{Z_{\Gamma}(T, V, N)}{\dim(\Gamma)} \cdot \chi_{\Gamma}(\boldsymbol{\alpha}). \tag{1}$$

Here Γ characterizes the multiplets, i.e. the irreducible representations of the symmetry group, $\dim(\Gamma)$ is the dimension of that representation, and χ_{Γ} is the corresponding group character defined by

$$\chi_{\Gamma}(\boldsymbol{\alpha}) \equiv \mathrm{tr}_{\Gamma}[\hat{R}(\boldsymbol{\alpha})] = \sum_{m} D^{\Gamma}_{mm}(\boldsymbol{\alpha}), \tag{2}$$

where $\boldsymbol{\alpha}$ denotes the set of group parameters and $\hat{R}(\boldsymbol{\alpha})$ represents an element of the symmetry group. By exploiting the orthogonality relation of the group characters,

$$\int \mathrm{d}\boldsymbol{\alpha} \mathscr{M}(\boldsymbol{\alpha}) \chi^{*}_{\Gamma}(\boldsymbol{\alpha}) \chi_{\Gamma'}(\boldsymbol{\alpha}) = \delta_{\Gamma\Gamma'}, \tag{3}$$

where $\mathscr{M}(\boldsymbol{\alpha})$ is the group measure, any partition function Z_{Γ} restricted to the states of a given irreducible representation Γ can be projected out of the generating function. Hence, the first step is always to calculate the generating function, which can be done very easily in most cases by using [24]

$$\tilde{Z}(T, V, \boldsymbol{\alpha}) = \mathrm{tr}[\mathrm{e}^{-\beta\hat{H} + \mathrm{i}\boldsymbol{\alpha}\mathbf{Q}}], \tag{4}$$

where $\mathbf{Q}$ is the set of generators of the symmetry group. This method has been widely used in treating both Abelian $U(1)$-symmetry groups like strangeness [31, 32] or baryon number [27] and non-Abelian symmetry groups

like $SU(2)$ *-isospin* [26] or $SU(3)$ *-color* [28]. Although, due to the lack of internal restrictions, the generating function diverges in the case of external quantum numbers like the angular momentum (where the set of eigenfunctions is labelled by $L = 0, \ldots, \infty$), we always will get finite expressions after the projection is applied. For convenience, the exploitation of the orthogonality relation (3) may be reformulated in terms of a projection operator $\hat{P}_\Gamma$, which singles out the contributions belonging to a fixed Γ when applied to the corresponding generating function. We will now shortly review this technique and adapt it to our needs.

2.2 Projection operators for isospin and angular momentum conservation

The generating function (1) together with the orthogonality relation (3) suggest the following form for a general projection operator onto an irreducible repre-sentation Γ of a finite and compact group:

$$\hat{P}_\Gamma = \dim(\Gamma) \int \mathrm{d}\boldsymbol{\alpha} \mathscr{M}(\boldsymbol{\alpha}) \chi_\Gamma^*(\boldsymbol{\alpha}). \tag{5}$$

The conservation of electric charge Q and isospin I are not independent from each other since in a system with vanishing strangeness and baryon number the Gell-Mann-Nishijima relation yields $Q = I_3$. Therefore, we have to perform a projection onto the third component of the isospin in order to take care of electric charge conservation. Translated into group theoretical language, the character contained in the projection operator has to be replaced by the single matrix element $D^I_{I_3, I_3}$. The detailed form of the components building the projection operator depends on the choice of group parameters $\boldsymbol{\alpha}$, which should be adjusted to the geometry of the system. For the projection on isospin we shall use Euler angles (α, β, γ), and for $I_3 = 0$ in particular we get

$$\begin{aligned} \dim(I) &= 2I + 1, \\ \mathscr{M}(\alpha, \beta, \gamma) &= \frac{\sin\beta}{8\pi^2}, \\ D^I_{0,0}(\alpha, \beta, \gamma) &= P_I(\cos\beta), \end{aligned} \tag{6}$$

where P_I is the Legendre polynomial of order I. It should be mentioned here that the group measure $\mathscr{M}$ is already normalized to the group volume. Finally, the whole projection operator can be written as

$$\hat{P}_{I, I_3 = 0} = \frac{2I + 1}{8\pi^2} \int_0^{2\pi} \mathrm{d}\alpha \int_0^{\pi} \mathrm{d}\beta \int_0^{2\pi} \mathrm{d}\gamma \sin\beta P_I(\cos\beta). \tag{7}$$

As the annihilation process takes place at rest, we assume the geometry of the resulting quantum gas to be approximately spherically symmetric. Hence the projection onto angular momentum eigenstates should not prefer a certain direction, and a projection on L rather than on L_3 should be sufficient. As a parametrization of the corresponding rotations in three dimensional space we choose the unit vector $\mathbf{n}$ of the rotation axis and the rotation angle ω ranging from 0 to π. Accordingly,

$$\begin{aligned} \dim(L) &= 2L + 1, \\ \mathscr{M}(\mathbf{n}, \omega) &= \frac{\sin^2\left(\frac{\omega}{2}\right)}{2\pi^2}, \\ \chi_L(\mathbf{n}, \omega) &= \frac{\sin(2L + 1)\,\frac{\omega}{2}}{\sin\left(\frac{\omega}{2}\right)}, \end{aligned} \tag{8}$$

leading to the angular momentum projector

$$\hat{P}_L = \frac{2L + 1}{2\pi^2} \int \mathrm{d}\mathbf{n} \int_0^{\pi} \mathrm{d}\omega \sin\left(\frac{\omega}{2}\right) \sin\left((2L + 1)\,\frac{\omega}{2}\right). \tag{9}$$

2.3 Calculation of the generating function

Simultaneous projection on isospin and angular momentum extends the generating function to

$$\begin{aligned} \tilde{Z}(T, V, \boldsymbol{\alpha}_I, \boldsymbol{\alpha}_L) &= \mathrm{tr}[\mathrm{e}^{-\beta\hat{H} + \mathrm{i}\boldsymbol{\alpha}_I \cdot \mathbf{I} + \mathrm{i}\boldsymbol{\alpha}_L \cdot \mathbf{L}}] \\ &= \mathrm{tr}[\mathrm{e}^{-\beta\hat{H} + \mathrm{i}(\alpha, \beta, \gamma) \cdot \mathbf{I} + \mathrm{i}\omega \cdot \hat{L}_3}]. \end{aligned} \tag{10}$$

In the last step we used the fact that, if there is no projection on a third component, then the character of a group can be expressed by the generator of the Cartan subgroup [33]. In order to work out the trace we choose as a set of basis functions the spherical harmonics,

$$|\mathbf{r}, k, l, m, t, t_3\rangle \equiv j_l(kr)\, Y_l^m(\theta, \phi) \cdot Y_t^{t_3}(\vartheta, \varphi), \tag{11}$$

where t and t_3 stand for the isospin and its third component, just as l and m stand for the angular momentum and its third component. Since the commutator $[\hat{L}, \hat{k}]$ does *not* vanish, angular momentum and total momentum cannot be conserved *exactly* at the same time, but in a canonical or grand canonical description energy and total momentum are conserved on the average automatically.

The trace is most easily evaluated in the occupation number representation. Let us, for simplicity, discretize the momentum spectrum and attach an index i to the various particle types ($i = 1, 2, \ldots, \nu$). Then, with n_i^{klm} being the number of particles of type i in a state with total quantum numbers k, l and m, we get

$$\begin{aligned} &\mathrm{tr}(\mathrm{e}^{-\beta\hat{H} + \mathrm{i}\boldsymbol{\alpha}_I I + \mathrm{i}\omega\hat{L}_3}) \\ &\quad = \mathrm{tr}(\mathrm{e}^{-\beta(\hat{h}_1 + \hat{h}_2 + \cdots) + \mathrm{i}\boldsymbol{\alpha}_I(\mathbf{i}_1 + \mathbf{i}_2 + \cdots) + \mathrm{i}\omega(\hat{l}_{3,1} + \hat{l}_{3,2} + \cdots)}) \\ &\quad = \sum_{\{n^{klm}\}} \prod_{k=0}^{\infty} \prod_{l=0}^{\infty} \prod_{m=-l}^{l} \left[\prod_{j=1}^{\nu} (D^{tj}_{t_3^j}(\boldsymbol{\alpha}_I))^{n_j^{klm}} \mathrm{e}^{\mathrm{i}\omega m \cdot n_j^{klm}} \right. \\ &\qquad \left. \times \left(4\pi \int_0^R \mathrm{d}r r^2 \mathrm{e}^{-\beta\varepsilon_j^k} [j_l(kr)]^2 \right)^{n_j^{klm}} \right], \end{aligned} \tag{12}$$

where $\{n^{klm}\}$ denotes all possible partitions $\{n_1^{klm}, n_2^{klm}, \ldots, n_\nu^{klm}\}$ of the various particle species on the state $|klm\rangle$. Using the Boltzmann approximation and

replacing the sum over momentum states by an integral we obtain

$$\begin{aligned}\mathrm{tr}(\cdots) &= \prod_l \prod_m \prod_{j=1}^{\nu} \exp\{D^{tj}_{t_3^j,t_3^j}(\alpha\beta\gamma)\cdot e^{i\omega m} 4\pi \int_0^R dr r^2\cdot(2\pi)^{-3} \\ &\quad \times \int d\mathbf{k} e^{-\beta\varepsilon_j(\mathbf{k})}[j_l(kr)]^2\} \\ &= \prod_l \prod_m \exp\left\{\sum_{j=1}^{\nu} D^{tj}_{t_3^j,t_3^j}(\alpha\beta\gamma) e^{i\omega m}\tilde{z}_1^j(T,V,l)\right\} \\ &= \exp\left\{\sum_{j=1}^{\nu} D^{tj}_{t_3^j,t_3^j}(\alpha\beta\gamma)\sum_{l=0}^{\infty}\chi_l(\omega)\tilde{z}_1^j(T,V,l)\right\}, \end{aligned} \tag{13}$$

where

$$\tilde{z}_1(T,V,l) = \frac{1}{2\pi^2}\int_0^R dr r^2 \int d\mathbf{k}\, e^{-\beta\varepsilon_j(\mathbf{k})} j_l^2(kr) \tag{14}$$

is a modified one-particle partition function, and $\chi_l(\omega)$ is given by (8). If we look at the infinite series

$$\sum_{l=0}^{\infty}(2l+1)\, j_l^2(z) = 1, \tag{15}$$

$\tilde{z}_1$ is seen to be simply related to the usual one-particle partition function,

$$\sum_{l=0}^{\infty}(2l+1)\tilde{z}_1(T,V,l) = \frac{V}{(2\pi)^3}\int d\mathbf{k} e^{-\beta\varepsilon(k)} = z_1(T,V). \tag{16}$$

In principle the generating function should also contain the degeneracy factors of quantum numbers which are not projected out, for example the spin factors. These factors can be put directly in front of the one-particle partition functions,

$$\tilde{z}_1(T,V,l) \mapsto (2S+1)\cdot\tilde{z}_1(T,V,l). \tag{17}$$

The evaluation of the function $\tilde{z}_1$ itself is discussed later.

2.4 *The projection mechanism*

In order to apply the projection operator for isospin or angular momentum, the exponential function has to be expanded into terms of fixed particle number n and it can be seen explicitly that a Gibbs factor for identical particles is always included automatically. In our model particles are "identical" if they belong to the same isospin multiplet and have the same internal quantum numbers and equal mass. Because we have classified the particles in multipletts with respect to the strong interaction, mass differences generated by the electromagnetic interaction do not show up here.

Isospin and angular momentum are independent quantum numbers so that one is allowed to apply the projection operators independently,

$$\hat{P}_{I,I_3}\hat{P}_L\cdot\tilde{Z}(T,V,\alpha,\beta,\gamma,\mathbf{n},\omega) = \sum_{n=0}^{\infty} G(I,I_3,n)\cdot G(T,V,L,n). \tag{18}$$

Let us first turn to the isospin projection acting on a term of the generating function with fixed particle number n. Then $G(I,I_3,n)$ consists of integrals of the following type:

$$\begin{aligned}\mathscr{I}_1 &= \frac{2I+1}{8\pi^2}\int_0^{2\pi} d\alpha \int_0^{\pi} d\beta \int_0^{2\pi} d\gamma \sin\beta P_I(\cos\beta) \\ &\quad \cdot D^{t^1}_{t_3^1,t_3^1}(\alpha\beta\gamma)\cdots D^{t^n}_{t_3^n,t_3^n}(\alpha\beta\gamma). \end{aligned} \tag{19}$$

The explicit form of the isospin matrix element is well known [34],

$$D^t_{t_3,t_3}(\alpha\beta\gamma) = \left(\frac{1+\cos\beta}{2}\right)^{t_3} P^{0,2t_3}_{t-t_3}(\cos\beta) e^{-it_3(\alpha+\gamma)} \tag{20}$$

with the Jacobi polynomial

$$\begin{aligned}P^{0,2t_3}_{t-t_3}(x) &= 2^{-t+t_3}\sum_{\nu=0}^{t-t_3}\binom{t-t_3}{\nu}\binom{t+t_3}{t-t_3-\nu} \\ &\quad \times (x-1)^{t-t_3-\nu}(x+1)^{\nu}. \end{aligned}$$

As the total isocharge vanishes, the sum of single particle isocharges must cancel likewise, and

$$t_3^1 + t_3^2 + \ldots + t_3^n = 0, \tag{21}$$

rendering the integrand independent of α and γ. In our approach, the multi-meson states consist of particles with isospin t equal to 0, 1/2 or 1, and the total isospin I is restricted to 0 or 1. In this special case, the projection integral (7) can be expressed in a compact way:

$$\mathscr{I}_1 = (2I+1)\cdot\left(\frac{1}{2}\right)^{\tilde{N}+1}\sum_{n=0}^{\tilde{N}}\binom{\tilde{N}}{n}\cdot\left[\frac{1-(-1)^{n+N_{1,n}+1+I}}{n+N_{1,n}+1+I}\right], \tag{22}$$

where

$$\tilde{N} = N_{1,c} + \frac{1}{2}N_{1/2}$$

and

$N_{1,n}$ = number of particles with (t,t_3) equal to $(1,0)$,

$N_{1,c}$ = number of particles with (t,t_3) equal to $(1,\pm 1)$,

$N_{1/2}$ = number of particles with t equal to 1/2.

We want to stress here, that the evaluation of (22) reveals simply the Clebsch–Gordan coefficient for the case that n single particle states with $(t^1,t_3^1),\ldots,(t^n,t_3^n)$ couple to a total isospin I and a vanishing third component $I_3 = 0$.

If we apply the angular momentum projection operator to the generating function, the ingredients of $G(T,V,L,n)$ are of the following form:

$$\begin{aligned}\mathscr{I}_2 &= \frac{(2L+1)}{2\pi^2}\int d\mathbf{n}\int_0^{\pi} d\omega \sin\left(\frac{\omega}{2}\right)\sin\left((2L+1)\frac{\omega}{2}\right) \\ &\quad \times \sum_{l_1=0}^{\infty}\cdots\sum_{l_n=0}^{\infty}\chi_{l_1}\cdots\chi_{l_n}\tilde{z}_1^1(T,V,l_1)\cdots\tilde{z}_1^n(T,V,l_n) \\ &= \sum_{l_1=0}^{\infty}\cdots\sum_{l_n=0}^{\infty}\tilde{z}_1^1(T,V,l_1)\cdots\tilde{z}_1^n(T,V,l_n) \\ &\quad \cdot\mathscr{I}_3(L,l_1,l_2,\ldots,l_n), \end{aligned} \tag{23}$$

where

$$\mathcal{J}_3(L, l_1, l_2, \ldots, l_n) = \frac{2(2L+1)}{\pi}$$

$$\times \int_0^\pi d\omega \sin\left(\frac{\omega}{2}\right) \sin\left((2L+1)\frac{\omega}{2}\right) \cdot \chi_{l_1} \cdots \chi_{l_n} \qquad (24)$$

is a well known expression in group theory: it yields the number of possibilities to form a state with fixed L out of n states with $l_1, \ldots, l_n$, respectively. The sums over the l-dependent modified one-particle partition functions are converging fast enough for a convenient computational exploitation.

To complete the set of tools needed to evaluate the full projection integral all that remains to be done is to evaluate the modified single particle partition functions $\tilde{z}_1$.

2.5 *The modified one-particle partition function*

The evaluation of the one-particle partition function generally depends on assumptions made about the shape of the interaction volume V. Not only for convenience but also for physical reasons a smooth surface of the interaction volume instead of a sharp edge would be desirable. In our further calculations we shall implement this feature by inserting a Gaussian cut-off into the volume-dependent part of the integrand and by shifting the upper integration limit from R to infinity:

$$\tilde{z}_1^i(T, V, l) = 4\pi \int_0^\infty dr r^2 e^{3r^2/2R^2} \int \frac{d\mathbf{k}}{(2\pi)^3} e^{-\beta\varepsilon^i(k)} [j_l(kr)]^2. \qquad (25)$$

The mean square radius is then given again by R. Now, the volume integral can be done analytically by writing

$$j_n(z) = \sqrt{\frac{\pi}{2z}}\, J_{n+1/2},$$

and using*

$$\int_0^\infty dr r e^{-\rho^2 r^2} J_{l+1/2}^2(kr) = \frac{1}{2\rho^2} \exp\left(-\frac{k^2}{2\rho^2}\right) I_{l+1/2}\left(\frac{k^2}{2\rho^2}\right). \qquad (26)$$

The remaining momentum integral then has to be evaluated numerically,

$$\tilde{z}_1(T, V, l) = \frac{R^2}{3} \int_0^\infty dk\, k\, e^{-\beta\sqrt{k^2+m_l^2} - k^2R^2/3} I_{l+1/2}\left(\frac{k^2R^2}{3}\right). \qquad (27)$$

In principle one could solve this integral analytically by using a series representation of the modified Bessel function. However, since the resulting series after momentum integration converges very slowly, this is not computationally convenient.

In Figs. 1a,b we show explicitly the lowest angular momentum contributions to the ordinary one-particle partition function. We note that in the relevant temperature and volume region mostly the $l = 1$ contribution dominates, and only for very small values of T and/or V the $l = 0$ partition takes over. For larger values of T and V the contributions from higher angular momenta increase in importance, as can be expected from the classical definition of the angular momentum, $\mathbf{l} = \mathbf{r} \times \mathbf{p}$ ($\langle p \rangle$ increases with T, $\langle r \rangle$ increases with V).

Since energy-momentum conservation forbids the decay of $p\bar{p}$ into a single pion, the quantity shown in Fig. 1 is only of academic interest. In Figs. 2a,b we show

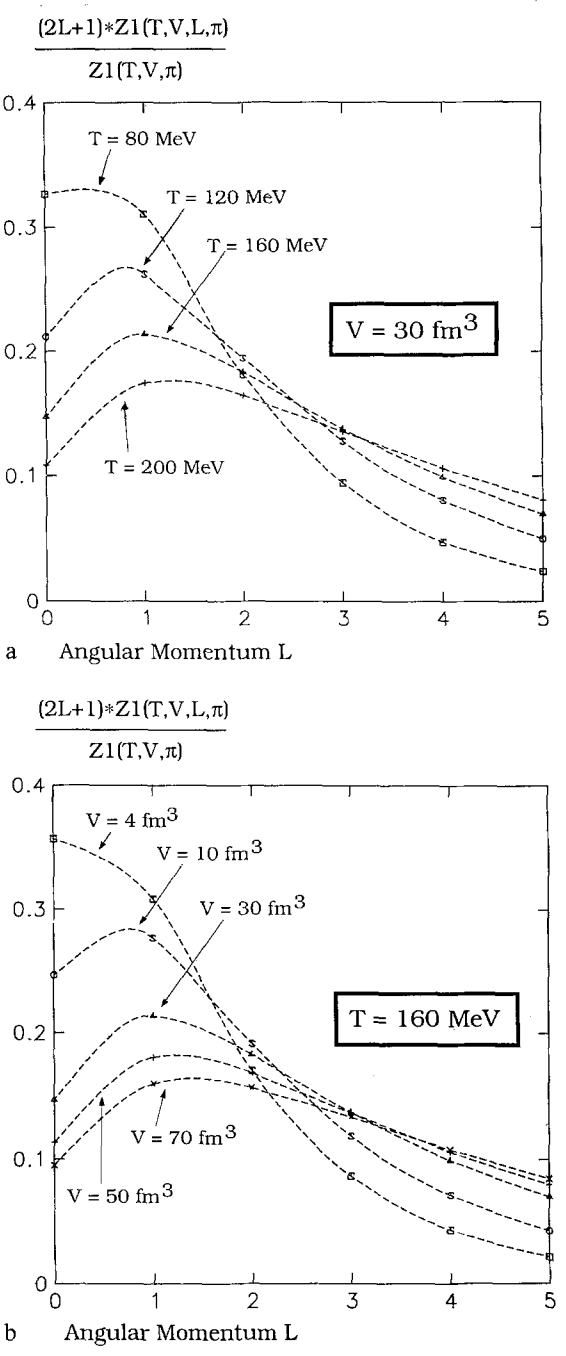

a

b

Fig. 1a,b. The modified one-pion partition function $\tilde{z}_1^\pi(T, V, l)$, multiplied with the degeneracy factor $(2l + 1)$ and normalized to the usual one-pion partition function $z_1^\pi(T, V)$, as a function of angular momentum, l, for various fireball volumes **a** and temperatures **b**

*see, e.g., G. N. Watson: A Treatise on the Theory of Bessel functions, Cambridge, 1922, 395(1)

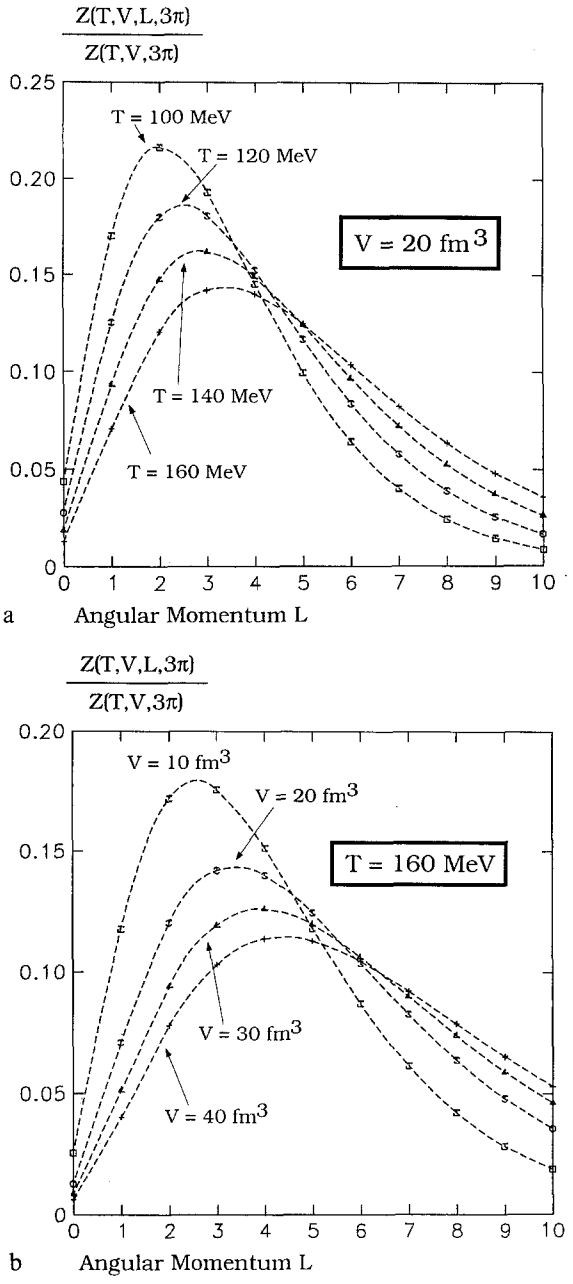

a

b

Fig. 2a,b. Normalized angular momentum partitions ($L = 1, \ldots, 10$) of the three-pion partion function $Z(T, V, 3\pi)$, for a fixed volume of 20 fm^3 at temperatures between 100 and 160 MeV **a** and for a fixed temperature of 160 MeV at volumes between 10 and 40 fm^3 **b** The degeneracy factor $(2L + 1)$ is already contained in $Z(T, V, L, 3\pi)$

the analogous decomposition of the 3-pion partition function $Z(T, V, 3\pi)$ into its angular momentum components $Z(T, V, L, 3\pi)$. The latter contain only those 3π-states which couple to a total angular momentum L, including the $(2L + 1)$ degeneracy factor. For simplicity, the conservation of additional quantum numbers is neglected here. The various contributions are normalized according to

$$\sum_{L=0}^{\infty} \frac{Z(T, V, L, 3\pi)}{Z(T, V, 3\pi)} = 1.$$

Again we see that non-zero values of L dominate the total partition function, with the peak value shifting to larger L as T and V increase.

Because for a n-pion system $L = J$, and because for $\bar{p}p$-annihilation at rest the total angular momentum is restricted to $J \leq 2$ (see Appendix), angular momentum conservation implies a very strong constraint on the partition function of such a system: all contributions in Fig. 2 with $L > 2$ have to be omitted.

3 Application to $\bar{p}p$-annihilation at rest

For convenience and because of the strong suppression of very massive particles in a thermodynamical description, the dilute quantum gas of our model will be assumed to consist only of the groundstate nonets of pseudoscalar and vector mesons. Note that we are considering annihilation at rest for which the possibility to excite heavy meson resonances is limited to a mass well below $2m_{\text{proton}}$.

First, in Sect. 3.1 we want to make some short remarks on the relevant quantum numbers of the system in its initial state (protonium) and its final state (multimeson gas). In Sect. 3.2 we investigate the partition function including all conservation laws on the one hand and compare it, on the other hand, with the partition function which contains only isospin- and strangeness conservation. The differences can be illustrated best by splitting the partition function into the various N-particle contributions. Some specific particle ratios are discussed in Sect. 3.3 where the deviations from the unconstrained behaviour caused by the exact quantum number conservation can be seen explicitly.

In Sect. 3.4 we confront our results with experimental data. Unfortunately, due to the focus on the microscopic features of annihilation in recent years, only very few (and rather old) inclusive data for $\bar{p}p$-annihilation at rest are available. We find that definite statements about the applicability and limits of our approach would require more inclusive data.

3.1 Internal and external quantum numbers

For the understanding of the annihilation process in the $\bar{p}p$ system a proper treatment of all conservation laws respected by the strong interaction is crucial. The quantum number combinations of the protonium can be classified in a spectroscopic notation, and for completeness a survey of the relevant S- and P-wave states is contained in the Appendix.

In this work, we will treat the conservation of all internal quantum numbers (baryon number, strangeness, electric charge or isospin) exactly. With regard to external quantum numbers, i.e. quantum numbers connected to spacetime symmetries, the usual conservation of total energy and momentum turns out to be insufficient. Since the initial state is also characterized by angular momentum and related discrete quantum numbers, the exact conservation of total angular momentum J, parity P, charge conjugation C and G-parity is a necessity.

In principle, once the angular momentum of a multimeson final state is determined, well known expressions for the P-, $C-$ and G-parity can be found in many textbooks (e.g. [35]). However, there are some states which require special treatment, namely those containing at least one KK^*-pair. Zero strangeness provided, there are two possibilities to construct a KK^* isospin eigenfunction: $(K^+, K^0) \otimes (\bar{K}^{0*}, K^{-*})$ or $(\bar{K}^0, K^-) \otimes (K^{+*}, K^{0*})$. In order to get also an eigenfunction of the C parity operator, we ought to make a superposition of the two isospin eigenfunctions, for example

$$\varphi(I=0, C=-1) = \sqrt{\frac{1}{4}} \left(|K^+ K^{-*}\rangle - |K^0 \bar{K}^{0*}\rangle + |\bar{K}^0 K^{0*}\rangle - |K^- K^{+*}\rangle \right).$$

Because of the factor $\sqrt{1/4}$, the contribution of this particular $K\bar{K}^*$-state to the partition function is reduced by a factor of one half, compared to the situation without C parity conservation. The G-parity of such a state can be fixed only after the decay of the kaon resonance.

Together with the generalized Pauli principle [35], some additional restrictions will be put on the number of available final states, for example

–two neutral pions always must have even orbital angular momentum,

$|\pi^0 \pi^0\rangle \rightsquigarrow L = 0, 2, 4, \ldots;$

– for two charged pions, the sum of total isospin and angular momentum must always be an even number;

– the $\eta\eta$-state must have even angular momentum, Ł = 0, 2, 4, ... ;
etcetera.

In general, the application of the generalized Pauli principle should not be restricted to two-particle states only, but with increasing particle number n its constraining power vanishes and we will therefore neglect the influence of the Pauli principle on states with n greater than two.

Putting all the selection rules together, those arising from internal conservation laws as well as those emerging from external invariance principles, we are now able to simulate the statistical behaviour of the $p\bar{p}$-annihilation system.

3.2 An analysis of the partition function

In order to get a feeling for the reliability of our results, let us have a closer look at the partition function first. Because computer time grows exponentially with N and because experimentally high N contributions to the final multimeson states are suppressed very strongly [36], we will limit ourselves to the contributions with $N \leq 7$ to the partition function. This turns out to be a good approximation for the small interaction volumes expected to occur in $\bar{p}p$-annihilation, if T is not too large.

In Figs. 3 and 4 the partition function has been split into the fractional N-particle contributions, that is $Z(T, V, N)/Z(T, V)$ (due to the explosion of numerical effort for large values of N, the denominator used for normalization in the figures contains actually only the sum of contributions from $N = 1$ through 7). In all cases we ensure strangeness, baryon number and electric charge conservation. In Figs. 3a–3c we impose additionally

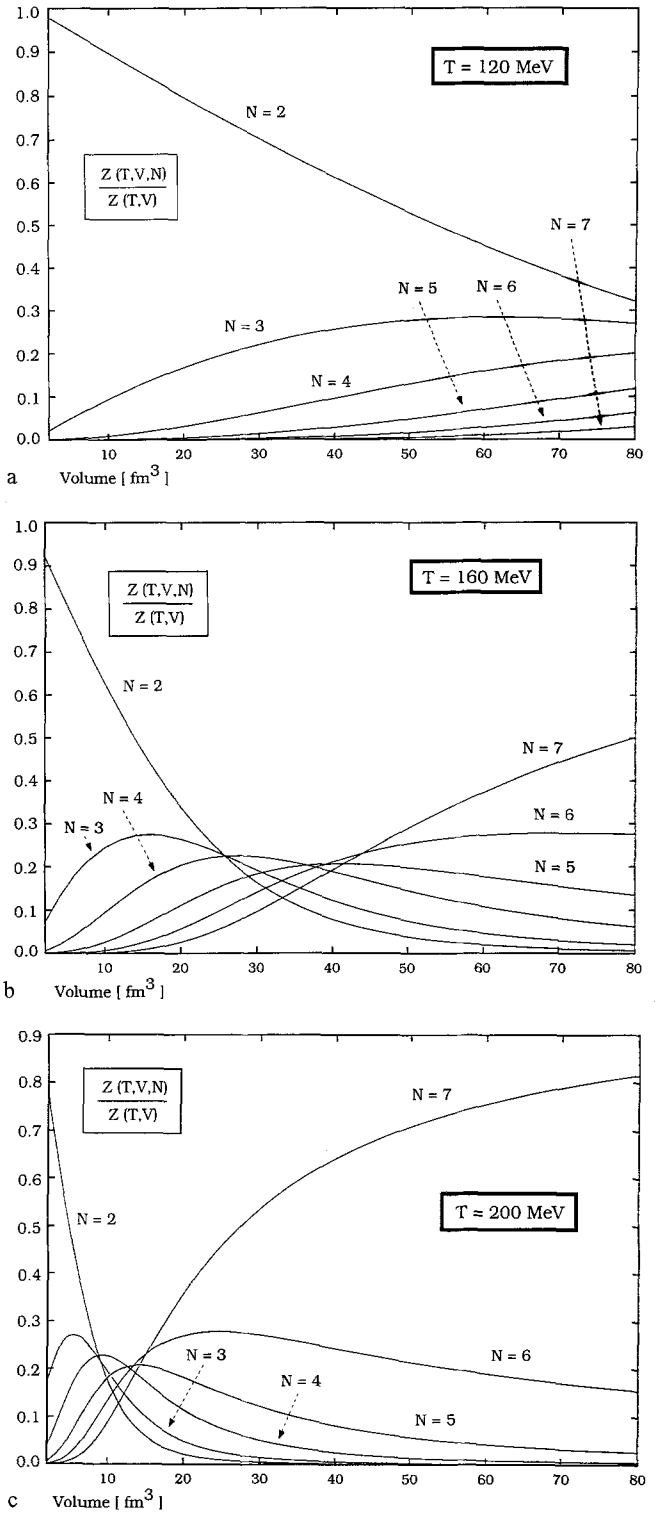

Fig. 3a–c. Fractional N-particle contributions to the meson gas partition function, $Z(T, V, N)/\sum_{N=1}^{7} Z(T, V, N)$, for **a** $T = 120$ MeV, **b** $T = 160$ MeV, and **c** $T = 200$ MeV. Only strangeness, baryon number, electric charge and isospin are conserved; the conservation of the external quantum numbers is not included here

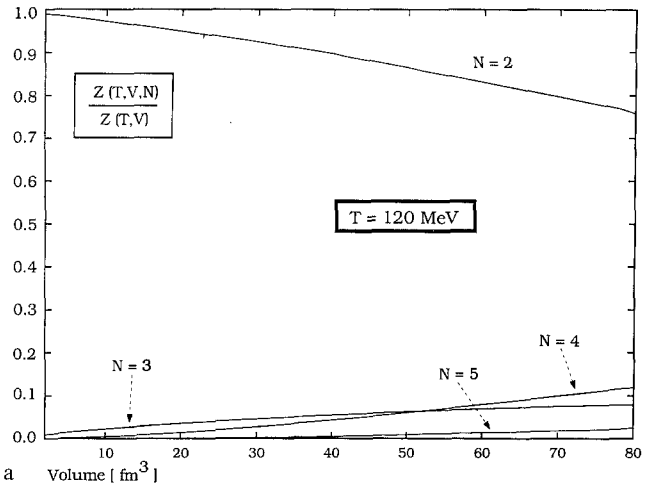

a

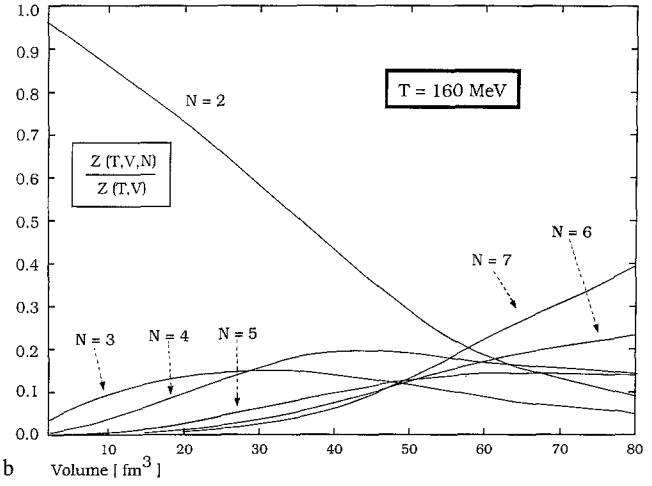

b

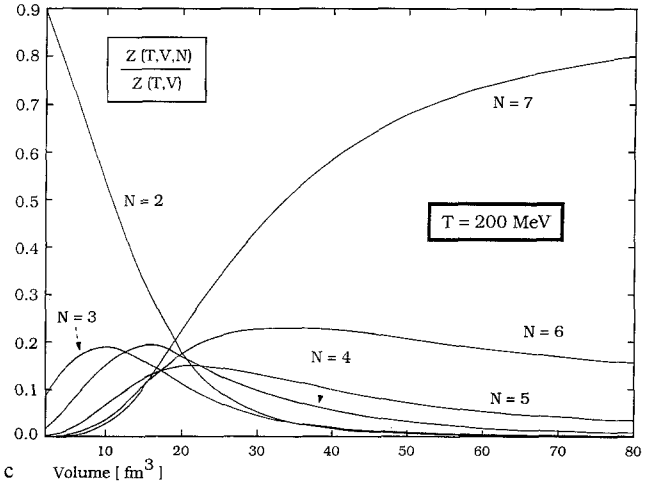

c

Fig. 4a–c. Same as Fig. 3, but now also including the exact conservation of the external quantum numbers

isospin conservation, and in Figs. 4a–4c also total angular momentum, P, C and G parity conservation. Comparing Fig. 3a with Fig. 4a, the difference is striking: for a temperature T of 120 MeV, the dominance of the two-particle contribution grows drastically if the external selection rules (ESR) are taken into account. This tendency also holds when the temperature increases, although for 200 MeV the two-particle dominance is restricted to small volumes. The main reason for this behaviour is obviously contained in the angular momentum projection mechanism: if N increases, the number of states which are forbidden due to the ESR restrictions is also growing, and very rapidly so. Of course, this will affect the particle ratios significantly, and as a first result we want to state that it is absolutely necessary to include the total angular momentum conservation and the ESR which come along with it.

As long as the interaction volume is smaller than about 20 fm^3, $\bar{p}p$ annihilation proceeds for temperatures up to 200 MeV mainly via two-meson states. As V increases, the terms with $N \geq 6$ become more and more important, especially as T also increases. For large values of VT^3 we approach the unconstrained limit. However, since experimental data show a strong suppression of the high N contributions [36], the acceptable physical region for the final multi-meson phase just before decoupling must be limited to rather small volumes. This finding is rather different to early approaches in the framework of thermodynamical models where rather large volumes had to be introduced [5, 9, 26, 37]. The reduction of the volume parameter in our model is essentially the consequence of the exact rather than average conservation of the quantum numbers of the annihilating system. The most important conservation law turns out to be the one for angular momentum.

3.3 Particle ratios

The usual method to extract particle multiplicities from the partition function is as follows: after assigning to every particle type i a chemical potential μ_i for book-keeping purposes, the multiplicities are obtained by calculating the derivative of the logarithm of the partition function with respect to these chemical potentials at $\mu_i = 0$:

$$\langle N_i \rangle = T \cdot \partial_{\mu_i} \ln[Z(T, V, B, S, I, \ldots, \mu_i, \ldots)]_{\mu_i = 0}. \qquad (28)$$

In Fig. 5a we show the primary π^0/π^+-ratio (i.e. before resonance decays), without angular momentum conservation (AMC) and associated ESR restrictions, but subject to S, B, I and I_3 conservation. In the unconstrained limit the ratio tends to 1. The behaviour in the domain of small volumes can be explained in the following way: the suppression of neutral pions at low T comes mainly from the I, I_3-conservation and the dominance of the two-particle states. As the production of heavy particles is suppressed, the dominant two-particle states are $|\pi^0\pi^0\rangle$ and $|\pi^+\pi^-\rangle$. The neutral pion suppression then originates in the Clebsch-Gordan coefficients of the two-pion isospin wavefunction. As T increases, more and more massive particles, e.g. the isospin singlets η, η', ω, ϕ, are produced together with a neutral pion in the two-particle channel, thus effectively removing the selection rule against neutral pion pairs. At high temperatures, this effect even makes the π^0-yield exceed the π^+-yield. Surely, this mechanism is at work also in states with $n > 2$, but the effect is strongly diminished with increasing n because the number of

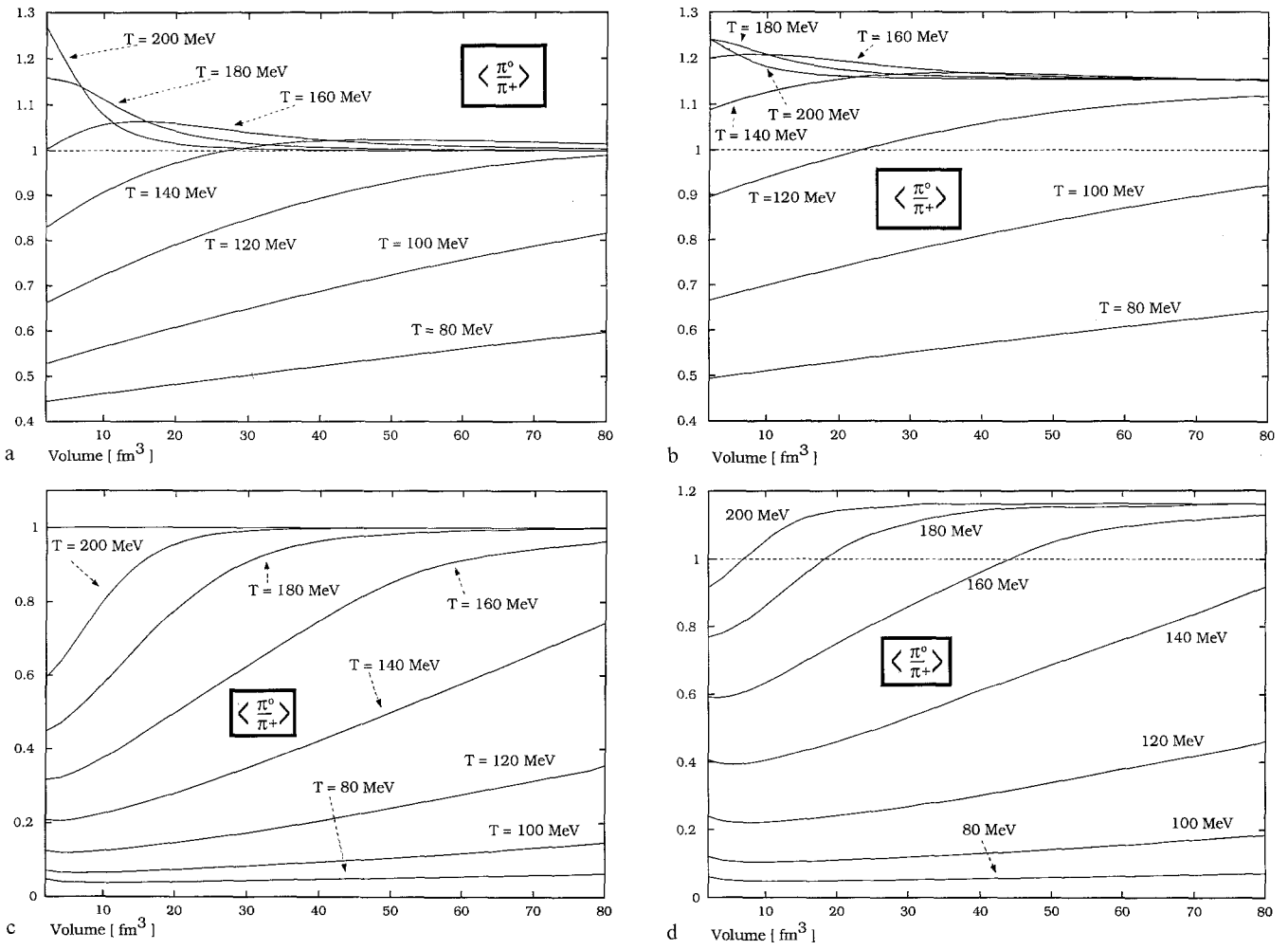

Fig. 5a–d. π^0/π^+-ratio as a function of the fireball volume, for several values of T. **a.** conservation of S, B, Q and I only, no resonance decay contributions; **b** same as **a**, but including resonance decay contributions; **c** all conservation laws included, but no resonance decay contributions; **d** same as c, but including resonance decay contributions

particle combinations, containing charged or neutral pions, grows with the nth power.

The situation changes drastically when angular momentum conservation and ESR are included, as can be seen from Fig. 5c. In all the following figures concerning AMC and ESR, the angular momentum distribution of the $\bar{p}p$-annihilation system at rest in liquid hydrogen is simulated (i.e. 92% S-wave and 8% P-wave, cf. Appendix). States like $\pi^0\pi^0$ or $\pi^0\eta$ are now forbidden in the dominant S-wave channel due to the violation of P parity. This leads to an overall suppression of the neutral pions, which is much stronger now than before: even for $T = 200$ MeV the ratio is clearly smaller than one.

All these effects are washed out to some extent once the decay of unstable resonances after freeze-out is taken into account, as shown in Figs. 5b and 5d. As is well known [38], these decays produce additional pions with a preference for neutral rather than charged ones. Due to this effect, the π^0/π^+-ratio exceeds unity by about 15% in the grand canonical limit.

In Fig. 6 we show the analogous results for the K^0/π^+ ratio. This ratio is not so much affected by AMC and by ESR restrictions (cf. Figs. 6a and c). The exact conservation of these quantum numbers leads to a slight overall suppression of strangeness production which can still be seen at rather large fireball volumes. The temperature dependence of the grand canonical (large V) limit of this ratio is, of course, due to the $K - \pi$ mass difference. In the region of very small volumes, an additional change in the shape of the curves can be noticed when AMC and ESR are included: the charged pions feel more restrictions than the kaons. For example, the final $\pi^+\pi^-$ state can only exist, if the S-wave annihilation starts from a $^{3,3}S_1$ state (see Table 1). From Figs. 6b and 6d we observe that resonance decays into (predominantly) pions and (more rarely) kaons shift all the curves downwards, in particular at high temperatures where resonances are important, but leave the shape of the volume dependence unaltered.

A further example for the striking impact of AMC and ESR is the ρ^0/π^+ ratio shown in Fig. 7. A remarkable feature of this ratio is that it seems nearly untouched by exact conservation of isospin and its third component, even for very low volumes, Fig. 7a. A deviation from the unconstrained limit arises only under the influence of AMC and ESR, shown in Fig. 7c. Again, resonance decays

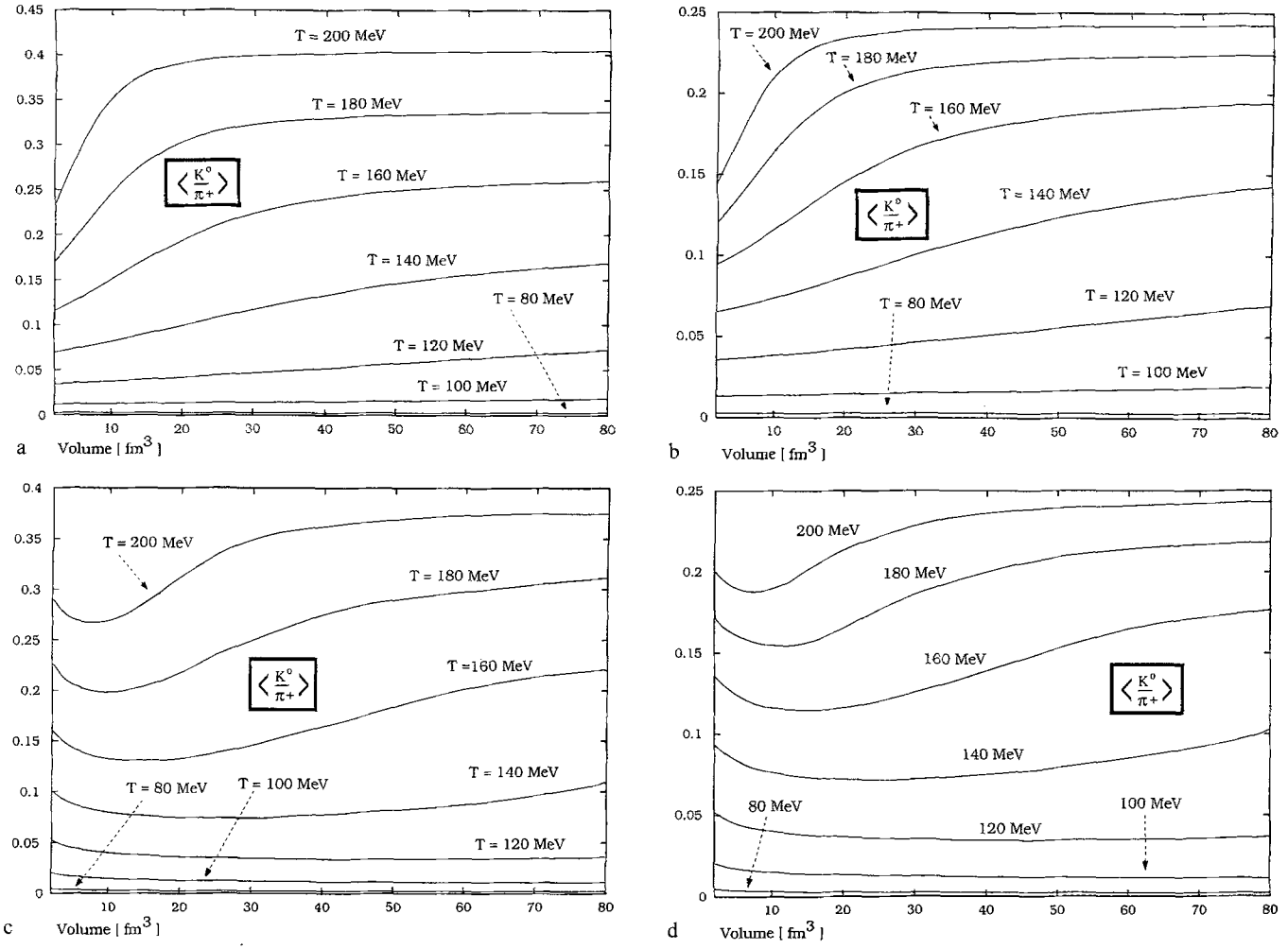

Fig. 6a–d. Same as Fig. 5, but for the K^0/π^+-ratio

Table 1. Conserved quantum numbers and corresponding probabilities of $p\bar{p}$ annihilation at rest in liquid hydrogen

$^{2I+1,2S+1}L_J$	C	P	CP	G	$P_{L,S,J,I}$
$^{1,1}S_0$	+	−	−	+	0.115
$^{3,1}S_0$	+	−	−	−	0.115
$^{1,3}S_1$	−	−	+	−	0.345
$^{3,3}S_1$	−	−	+	+	0.345
$^{1,1}P_1$	−	+	−	−	0.01
$^{3,1}P_1$	−	+	−	+	0.01
$^{1,3}P_0$	+	+	+	+	0.0033
$^{1,3}P_1$	+	+	+	+	0.01
$^{1,3}P_2$	+	+	+	+	0.0166
$^{3,3}P_0$	+	+	+	−	0.0033
$^{3,3}P_1$	+	+	+	−	0.01
$^{3,3}P_2$	+	+	+	−	0.0166

shift the curves downwards as a whole but do not change the qualitative dependence on T and V, Figs. 7b and d. We want to emphasize here, that the π^+-multiplicity in Figs. 7b and d contains the yield from all resonance decays, including the ρ^0 decay. This is done to facilitate comparison with the data where usually the exclusive and inclusive multiplicities are extracted from different measurements.

The η/π^0 ratio also seems to be rather unsensitive to exact quantum number conservation, see Figs. 8a and c. However, the ratio decreases slightly if AMC and ESR are taken into account, at least for small values of V. This behaviour originates in the fact that several two-particle states containing an η (e.g. $\pi^0\eta$, $\eta\eta$, and $\eta\eta'$) are now forbidden in the S-wave, and this effect is even stronger than the π^0-suppression in this region, although not by very much. It should be mentionend that the η/π^+ ratio would provide a much more sensitive test of the influence of AMC and ESR: since charged pions are only weakly affected by the external constraints, the strong suppression effect on the η's would not be nearly cancelled in such a ratio. Unfortunately, no such data seem to be presently available.

From Fig. 8b one observes that without AMC and ESR constraints the resonance decays (including the η decay) drastically change the picture, resulting in a completely different volume dependence. At higher temperatures both the η yield and the π^0 yield from resonance decays increase, and the curves shown in Fig. 8b reflect the

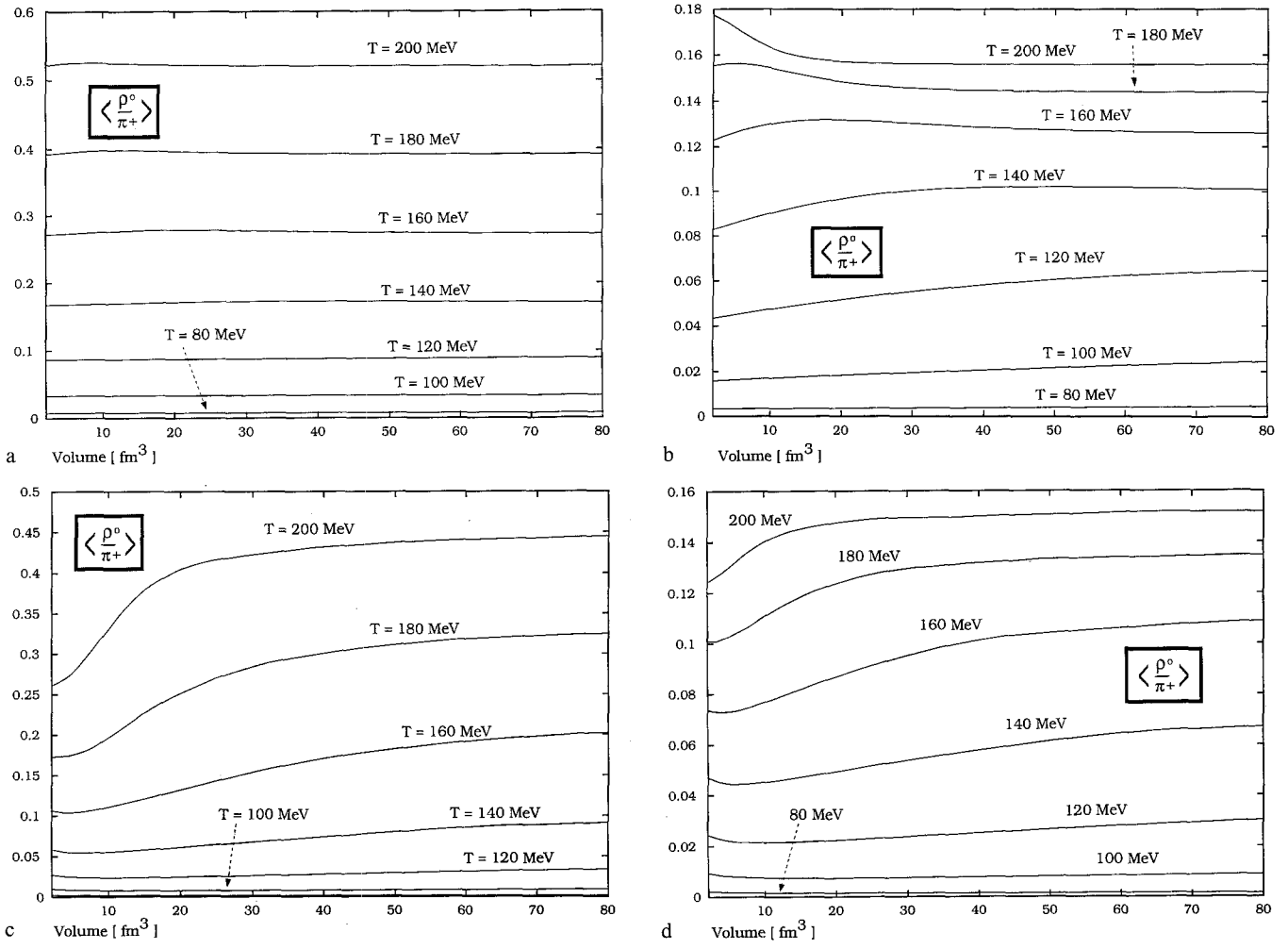

Fig. 7a–d. Same as Fig. 5, but for the ρ^0/π^+-ratio. In **b,d** the denominator also includes the pions from the ρ^0 decays

intricate interplay between these two effects. No such strong resonance decay effect on the shape of the curves is seen once AMC and ESR are included: due to the lack in the restricted partition function of many two-particle states containing an η, the effect of increasing η's at higher T is reduced, and the only remaining effect is an overall downward shift of the ratio by the resonance decay pions in the denominator.

3.4 Comparison with experimental data

The available amount of inclusive data for $\bar{p}p$-annihilation *at rest* is unsatisfactorily small, and no data for ratios like π^0/π^+ or K^0/π^+ can be found in the literature. Thus we are forced to try to extract these ratios from data on $\bar{p}p$-annihilation *in flight* [39]–[46] by extrapolating to $P_{\text{lab}} = 0$ (cf. Fig. 9), which turns out to be very difficult for the π^0/π^+ ratio because just in the region of very low P_{lab} the P-wave contribution to the $\bar{p}p$-compound changes very drastically [15], and so does the ratio. This behaviour originates in the strong dependence of the π^0-yield on the partial wave distribution: while some states containing neutral pions, like $\pi^0\pi^0$, $\pi^0\eta$ or $\pi^0\eta'$, are forbidden in the S-wave state of the $\bar{p}p$-system, they are allowed in the P-wave contribution. Since in our calculations the relative S- and P-wave contributions were fixed at 92% and 8%, respectively, our ratios don't reflect this sensitivity to a change in the partial wave contributions. On the other hand, not enough information is available for reliably modelling this change as a function of P_{lab}. Therefore it would be very desirable to have some data for the π^0/π^+-ratio for $\bar{p}p$-annihilation *at rest*, where the various partial wave contributions can be fixed experimentally. Referring to our results (cf. Fig. 5c), one can say that in the case of annihilation at rest in liquid hydrogen this ratio (only primary particles) should *always* be smaller than 1, and as our curves are very sensitive to the macroscopic parameters V and T, such a measurement can be expected to yield severe restrictions on the allowed range for these parameters.

More reliable is an extrapolation of the K^0/π^+-ratio, where the data seem to indicate a value of about 0.02 at rest, Fig. 9. Compared to our results this would suggest a rather low but not unreasonable temperature of about 100 MeV. The same tendency holds true if we compare

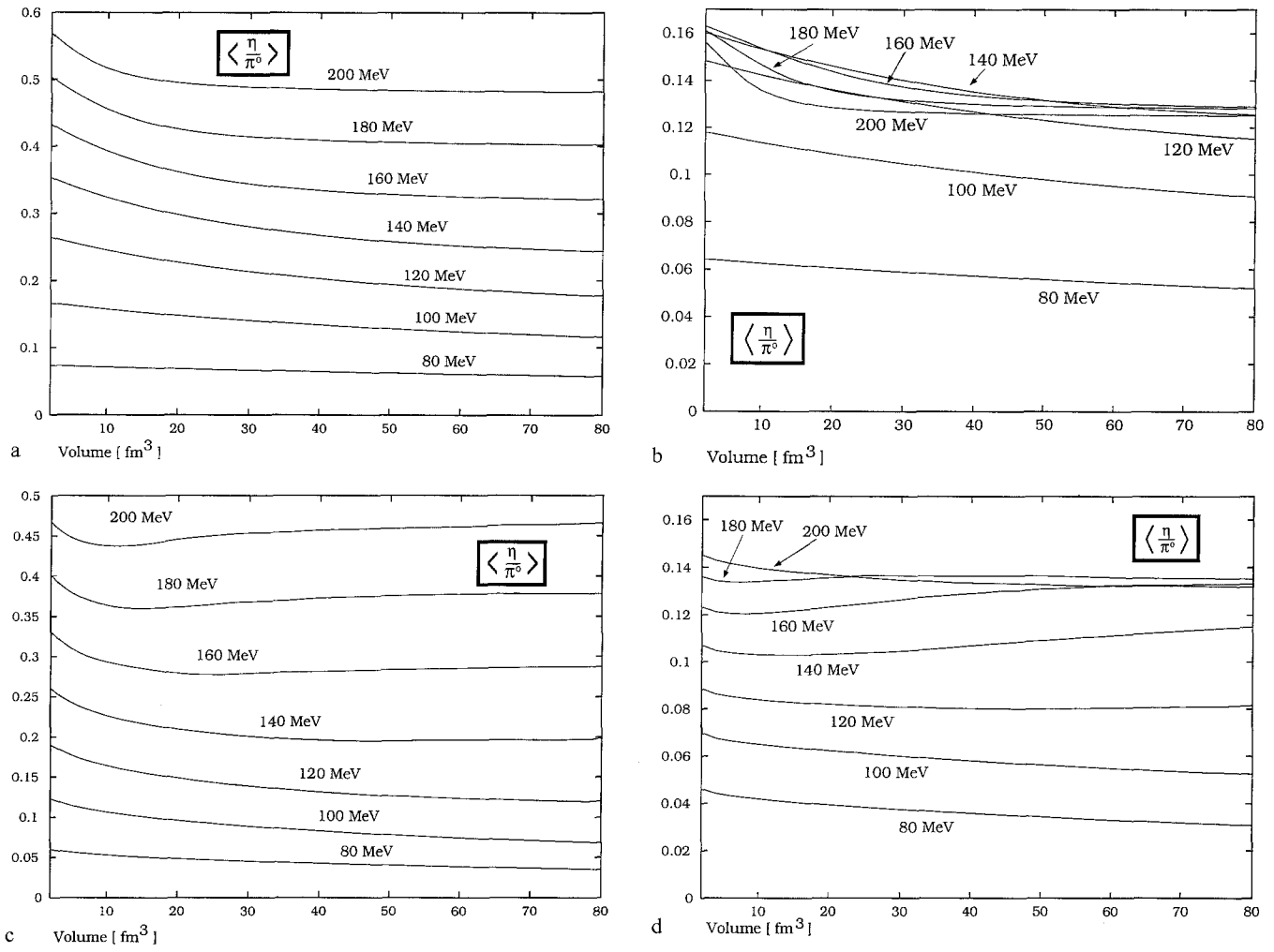

Fig. 8a–d. Same as Fig. 5, but for the η/π^0-ratio. In b,d the denominator also includes the neutral pions from η decays

our computed η/π^0 ratio (Fig. 8d) with the measured value of $(3.67 \pm 0.41) \times 10^{-2}$ [47, 48]. On the other hand, such a low temperature would produce at most two pions on the average because resonance production is strongly suppressed. This might be a hint that the pion data contain additional contributions from the decay of heavier resonances which are not yet contained in our model.

4 Conclusions

Let us briefly summarize the most important theoretical aspects of this work. As far as we know the straightforward formalism for including total angular momentum conservation into a thermodynamical model, which was presented in this paper and applied to $\bar{p}p$-annihilation at rest, is a new development. In order to achieve that goal we had to use an extension of the projection operator method to non-Abelian symmetry groups and further generalize it to include discrete quantum numbers corresponding to external symmetries. We have included all the relevant quantum numbers and found for small thermodynamic systems strong deviations from the unconstrained limit where these quantum numbers are only conserved on the average.

Most importantly we found that the two-particle contribution completely dominates the total meson gas partition function in the temperature and volume region relevant for $p\bar{p}$ annihilation. Since these two-particle channels experience particularly strong constraints from the conservation laws, all particle ratios turn out to be rather sensitive to the *exact* quantum number conservation.

In particular the production of neutral pions and η mesons is strongly influenced by *exact* conservation of the angular momentum and the connected parity quantum numbers C, P and G. Even for $T = 200$ MeV the ratio of π^0/π^+ changes by about 50% at small fireball volumes, and before resonance decays it is always smaller than one. Resonance decays change these results by about 10–15%, but the qualitative features are preserved. Kaon production, on the other hand, is not very much restricted by the conservation laws.

At this place we want to make a short remark on the temperature. Although the temperature range resulting from our calculations is of about the same order as the critical temperature T_c for the expected phase transition to

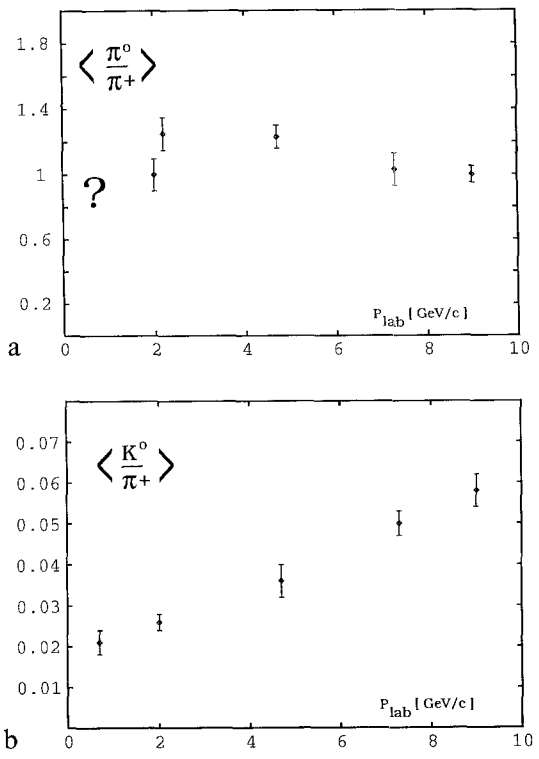

Fig. 9a,b. Experimental data for $p\bar{p}$-annihilation in flight for small $\bar{p}$ laboratory momenta (from [39–46]). **a** π^0/π^+; **b** K^0/π^+

the quark-gluon plasma, we would like to avoid speculations on such a phase transition in the $\bar{p}p$ system (as e.g. suggested in [26]). It is, however, true that in order to justify our treatment we have to assume some intermediate state resembling very much an ideal quantum gas, and that thermal equilibration must be somehow produced by an unknown microscopic mechanism in the annihilation/particle-creation process. The lifetime of the hadron gas itself is much too short for thermal equilibration [26, 29]. Yet since the microscopic properties of the intermediate kinetic state cannot be treated in the framework of a statistical model, a discussion about the origin of thermal equilibrium is rather academic, and the temperature T should simply be considered as a parameter which controls energy conservation on the average, nothing more.

For a comprehensive test of this constrained statistical approach more inclusive data for $\bar{p}p$-annihilation at rest are needed, particularly for the production of charged pions and kaons. We hope that our model calculations stimulate further experimental efforts in this direction. Further information is expected from the analysis of two- and three-particle flavor correlations. Work in this direction within the model presented in this paper is in progress.

Acknowledgements: We are grateful to Prof. W. Weise for stimulating comments on an early version of this paper. U. Heinz acknowledges support of his research by Deutsche Forschungsgemeinschaft (DFG), Bundesministerium für Forschung und Technologie (BMFT), and Gesellschaft für Schwerionenforschung (GSI). He thanks the members of the Institute for Theoretical Physics in Santa Barbara for their nice hospitality; his stay there was supported by the National Science Foundation under grant No. PHY89-04035.

Appendix: Quantum numbers of the $\bar{p}p$ system

In many experiments a liquid hydrogen target is used to deaccelerate the antiproton before annihilation; in this situation the system annihilates with 92% probability from the S-wave state ($L = 0$) and with 8% from the P-wave ($L = 1$), as can be checked by coincidence measurements of the X-rays from the preceding electromagnetic cascade in the $\bar{p}p$ atom [49]. These numbers are used in order to obtain the probabilities of all the possible quantum number combinations, shown in Table A.1 in a spectroscopic notation.

References

1. C. Ghesquière et al.: Symp. on NN̄-Interactions. CERN 74-18, Genf (1974)
2. J. Roy: in Proc. of the Fourth International Symposium on NN̄ Interactions. Syracuse University (1975)
3. H. Koppe: Z. Naturforschung 3A (1948) 251; Phys. Rev. 76 (1949) 688
4. E. Fermi: Progr. Theor. Phys. 5 (1950) 570
5. W.H. Barkas et al.: Phys. Rev. 105 (1957) 1037
6. V.M. Maksimento: Soviet Phys. JETP 6 (1958) 180
7. N. Yajima K. Kobayakawa: Progr. Theor. Phys. 19 (1958) 192
8. F. Cerulus: Nuovo Cimento 14 (1959) 827
9. M. Kretzschmar: Ann. Rev. Nucl. Sci. 11 (1960) 1–40
10. B. May et al.: Phys. Lett. 225B (1989) 450
11. E. Aker et al.: Phys. Lett. 260B (1991) 249
12. M. Mayurama, T. Ueda: Nucl. Phys. A364 (1981) 447
13. J. Vandermeulen: Z. Phys. C37 (1988) 563
14. C.B. Dover, T. Gutsche, M. Maruyama A. Fäßler: Prog. Part. Nucl. Phys. 29 (1992) 8
15. S. Mundigl, M.V. Vacas, W. Weise: Nucl. Phys. A523 (1991) 499
16. V.B. Magalinskii, Ya.P. Terletskii: Soviet Phys. JETP 5 (1957) 483
17. A. Pais: Ann. Phys. (N.Y.) 9 (1960) 548
18. F. Cerulus: Nuovo Cimento Suppl. 15 (1960) 402
19. Z. Koba, S. Takagi: Noouvo Cimento 18 (1960) 608
20. F. Cerulus; Nuovo Cimento 22 (1961) 958
21. B. May et al.: Z. Phys. C46 (1990) 191
22. B. May et al.: Z. Phys. C46 (1990) 203
23. R. Adler et al.: Phys. Lett. 267B (1991) 154
24. K. Redlich, L. Turko; Z. Phys. C5 (1980) 201
25. L. Turko: Phys. Lett. B104 (1981) 153
26. B. Müller, J. Rafelski: Phys. Lett. 116B (1982) 274
27. R. Hagedorn, K. Redlich: Z. Phys. C27 (1985) 541
28. Th. Elze, W. Greiner: Phys. Rev. A33 (1986) 1879
29. J.H. Kim, H. Toki; Progr. Theor. Phys. 78 (1987) 616
30. V.B. Magalinskii, Ya.P. Terletskii: Soviet Phys. JETP 2 (1956) 146
31. P. Koch et al.: Phys. Lett. B123 (1983) 151
32. C. Derreth et al.: Phys. Rev. C31 (1985) 1360
33. W. Greiner, B. Müller: Quantenmechanik, Teil 2: Symmetrien. p. 408 Frankfurt: Harry Deutsch 1990
34. F. Cerulus: Nuovo Cimento 19 (1961) 528
35. W.M. Gibson, B.R. Pollard: Symmetry principles in elementary particle physics, chapts. 7 and 8. Cambridge University Press 1976
36. Compilation of cross-sections III: p and $\bar{p}$ induced reactions, CERN-HERA 84-01, Genf (1984)
37. J. McConnell, J. Shapiro: Nuovo Cimento 28 (1963) 1272

38. J. Sollfrank, P. Koch, U. Heinz: Z. Phys C52 (1991) 593
39. R. Hamatsu et al.: Nucl. Phys. B123 (1977) 189
40. B.S. Chaudhary et al.: Symp. on NN̄-Interactions. CERN 74-18, Genf (1974)
41. T. Fields et al.: in: Symp. on NN̄-Interactions, CERN 74-18, Genf (1974)
42. J. Fry: in: 4th Int. Symp. on Multiparticle Hydrodynamics, Pavia (1973)
43. S. Barish et al.: Phys. Rev. D9 (1974) 2689
44. G.D. Patel et al.: Z. Phys. C12 (1982) 189
45. M. Markytan et al.: Nucl. Phys. B143 (1978) 263
46. A.M. Cooper et al.: Nucl. Phys. B136 (1978) 365
47. M. Chiba et al.: Phys. Rev. D39 (1989) 3227
48. G. Backenstoss et al.: Nucl. Phys. B228 (1983) 424
49. M. Doser et al.: Nucl. Phys A 486 (1988) 493